Mapping and ablation of atrial tachyarrhythmias : from signal to substrate

Groot, N.M.S. de

chapter

12

Ablation of Focal Atrial Arrhythmia In Patients with Congenital Heart Defects after Surgery: The Role of Circumscribed Areas with Heterogeneous Conduction

Natasja M. S. de Groot, Wing King Chan, Nico A. Blom,
Maurits Wijffels, Ernst E. Van der Wall, Martin J. Schalij

Abstract

Background: In patients late after surgical repair of congenital heart disease (CHD), areas with abnormal electrophysiological properties may either serve as slow conducting pathways within a macro-reentrant circuit or may be the source of focal atrial tachycardia (FAT). The role of these abnormal areas during FAT was evaluated prior to ablation.

Methods and Results: Electro-anatomical activation mapping of 62 atrial tachycardia (AT) was performed in 43 consecutive patients (37 ± 12yrs) after surgical repair of CHD. The mechanism of AT was scar related intra-atrial reentry (IART: n = 27), cavo-tricuspid related atrial flutter (AFL: n = 21), atrial fibrillation (AF: n = 2) or focal AT (FAT: n = 10). During IART, channels of slow conduction could be identified in all patients. Subsequent ablation was directed at connecting 2 non-conductive borders. The site of origin during FAT showed fractionated potentials and/or continuous electrical activity. Area ablation, directed at isolating the source area, resulted in termination of FAT in all cases. In 2 patients, ablation of an area showing continuous electrical activity giving rise to fibrillatory conduction resulted in termination of AF. Ablation of IART was successful in 70%; AFL and FAT were successfully ablated in all patients. No complications were observed.

Conclusion: AT in patients with surgically corrected CHD, although most often caused by a macro-reentrant mechanism, is the result of a focal mechanism in some patients. Areas of abnormal conduction may not only serve as a zone of slow conduction within a macro-reentrant circuit but also as the site of origin of a focal atrial arrhythmia. Catheter ablation directed at “source isolation” is effective in eliminating FAT in patients with CHD.

Introduction

Recurrent atrial tachycardia (AT) late after corrective- or palliative surgery in patients with complex congenital heart disease (CHD) contribute considerably to the morbidity and mortality of this group of patients.[1] AT in CHD patients are most often macro-reentrant tachycardia including cavo-tricuspid isthmus dependent atrial flutter, atrial fibrillation or intra-atrial re-entrant tachycardias.[2;3] In some patients however, AT may be caused by a focal mechanism.

Viable myocardial fibers embedded within areas of scar tissue play a pivotal role in initiation and perpetuation of macro-reentry tachycardias.[4;5] However, these abnormal areas may also give rise to AT of focal origin. So-far, focal mechanisms underlying post-operative AT have been rarely reported.

Catheter ablation may be a curative treatment for AT in CHD patients. For selection of the optimal ablation strategy it is essential to discriminate between the various mechanisms of post-operative AT.[2;3] Detailed mapping of the activation sequence during AT is therefore essential. Catheter ablation has evolved as an effective treatment modality for AT in patients with CHD due to the introduction of 3-dimensional endocardial mapping techniques. These mapping techniques have not only been used to unravel the mechanism of AT but also to establish criteria for distinguishing scar tissue from viable tissues.[4] However, despite the use of advanced mapping techniques catheter ablation of post-operative AT remains time-consuming and difficult.

The goal of this study was to unravel the mechanism of post-operative AT in a cohort of patients with surgically corrected CHD referred for catheter ablation and to study the location of the arrhythmogenic substrate and electrogram morphology at sites where ablation resulted in termination of the AT. In patients with AT of focal origin, we analyzed the role of localized areas of conduction abnormalities in perpetuation of AT.

Tabel 1

Congenital Heart Defect	Major Surgical Procedure	Diagnosis
TGA	Mustard	IART
TGA	Mustard	IART
TGA + PS	Mustard	IART
TGA + PS	Mustard	IART, IART
TGA + VSD	Mustard, Jatene	AFL (2), FAT, AF
TGA + TA + PA	Fontan	IART
TGA + TA + PS	Fontan	IART
TGA + TA + PS	Fontan	IART
TGA + MonoV + PS	Fontan	IART
TGA + MVA + PS	Fontan	IART
TGA + TA + PS + ASD	Fontan	IART, FAT
cc'TGA + MVA + PS	Fontan	IART
ccTGA + VSD + PS	LV-PA conduit	FAT (2), AFL
ccTGA + VSD + PS	modified B.S	IART (2)
TA + PS	Fontan	IART (3), FAT (2), AF
TA + ASD + PS	Fontan	AFL
TA + ASD + PS + VSD	Fontan	IART
monoV + monoA + TGA + PS	Fontan	IART (3), FAT
others (MVD, SV defect + anomalous PV return, AoS, AVSD,VSD, coarctation of aorta) (N = 9)	valve-replacement, closure defects	IART (4), AFL (5), FAT
ASD, (N = 8)	closure defect	AFL (3), IART (2), FAT (2)
ToF, (N = 8)	ToF correction	AFL: 9

TGA = transposition great arteries, ccTGA = congenital corrected TGA, PS = pulmonary stenosis, PA = pulmonary atresia, MVA = mitral valve atresia, TA = tricuspid atresia, VSD = ventricular septal defect, ASD = atrial septal defect, mono-V = mono-ventricle, mono-A = mono-atrium, Aos = aorta stenosis, SV = sinus venosus defect, PV = pulmonary veins, AVSD = atrio-ventricular septal defect, ToF = tetralogy of Fallot, B.S = blalock-Hanlon shunt, LV-PA = left ventricle – pulmonary artery.

Methods

Patient Population

Consecutive patients (n = 43, 21 male, 37 ± 12 (16-63) yrs, Table 1) referred for ablation of AT after surgical repair of CHD were included in this study. Data regarding underlying CHD and previous surgical procedures were obtained from hospital records. All patients underwent full cardiac evaluation prior to ablation including 24-hour Holter monitoring, echocardiography and a diagnostic electrophysiological study.

Mapping Procedure

Mapping was performed using a 3-D electro-anatomical mapping system (CARTO™, Biosense-Webster, Diamond Bar, CA, USA). A detailed description of the underlying technology of electro-anatomical mapping procedures has been given previously.[6;7] A 7F Navistar (4mm tip, 2 bipolar electrode pairs, inter-electrode distance 2 mm, Biosense-Webster, USA) was used for mapping and ablation. Bipolar electrograms were filtered at 10-400Hz. A bipolar atrial electrogram recorded by a 6F diagnostic catheter (Biosense-Webster) positioned in the RA served as a temporal reference. A reference sensor taped on the back served as a location reference.

If AT was not present at the onset of the procedure, it was induced using programmed electrical stimulation. 3-D bipolar activation and voltage maps were constructed during AT to 1) identify the underlying mechanism, and 2) select target sites for ablation. The local activation time was determined by automatically marking the earliest onset of each bipolar potential. If necessary, markings were adjusted manually. The peak-to-peak amplitude of the largest bipolar electrogram was used to construct colour coded voltage maps. Based on these maps, areas of scar were delineated using a cut-off value of 0.1 mV.[4] In case of fractionated potentials, the peak-to-peak amplitude of the largest deflection was measured.

Classification of Atrial Tachycardia

Based on the activation maps, three different types of AT were distinguished:

1) *typical atrial flutter (AFL):* a single (counter)-clockwise, cavo-tricuspid isthmus dependent macro-reentrant circuit,[8] 2) *intra-atrial reentrant atrial tachycardia (IART):* a macro-reentrant tachycardia involving scar tissue, suture lines or prosthetic materials,[9;10] 3) *focal atrial tachycardia (FAT)*: electrical activation originating from a small, circumscribed region from where it expands centrifugally to the remainder of the atria. There is no wavefront circulating around a macroscopic anatomical structure, a functional or structural line of conduction block. [8]

Ablation Procedure

After mapping, a radiofrequency catheter ablation procedure was performed. At each site, radio frequency current was applied for 60 seconds (tip temperature set at 70°C, maximum output 50W).

In all patients, success was defined as termination during ablation and non-inducibility. In addition, in patients with AFL and IART creation of a line of conduction block was assessed over respectively the cavo-tricuspid isthmus and between anatomical structures, scar tissue or prosthetic materials.

Statistical Analysis

All data were expressed as mean value ± SD. Statistical significance was defined as $P<0.05$.

Results

Sixty-two different AT were mapped and ablated in 43 patients (table I). The interval between the first surgical procedure and AT was 16 ± 2 (1-41) yrs. Because of recurrent or new AT, 8 patients underwent more than one ablation procedure (5 patients: 2 procedures, 2 patients: 3 procedures, 1 patient: 5 procedures). In the majority of AT (n = 48, 77%), mapping revealed the presence of a macro-reentrant arrhythmia (AFL: n = 21, 34%, IART: n = 27, 44%).

Typical Atrial Flutter

Twenty-one activation maps demonstrated a typical AFL (CL = 291 ± 87, (200-530) ms). A bi-directional conduction block after construction of a linear lesion at the cavo-tricuspid isthmus was assessed in all patients. In two patients, 2 ablation procedures were performed because of AFL recurrences.

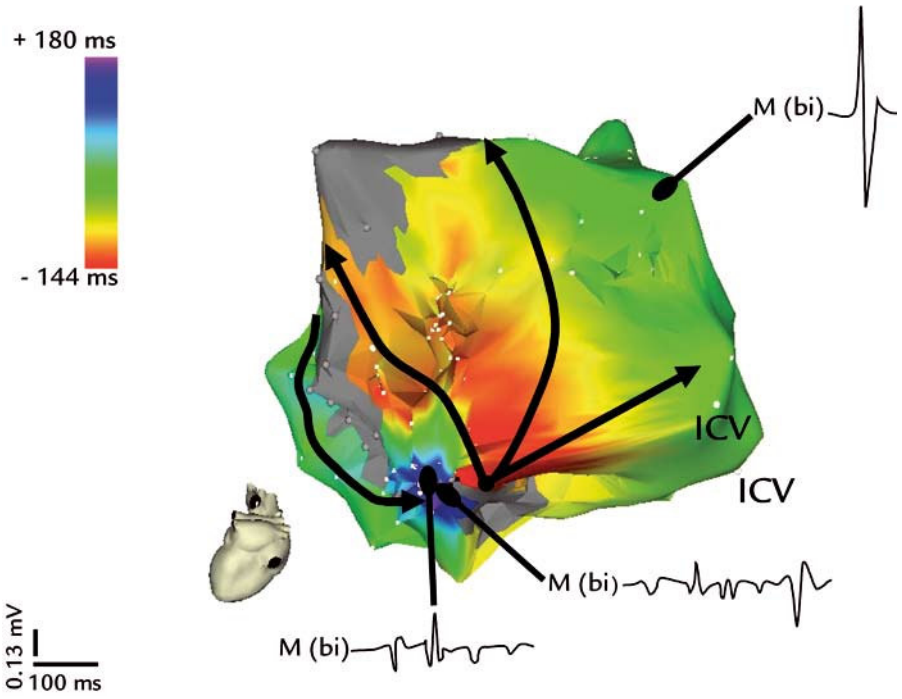

Figure 1.

Color coded activation map recorded during IART (CL = 324 ms) in a patient with Fontan circulation. The wavefront (black arrows) circulated around a large area of scar tissue (grey colour, delineated using a bipolar cut-off value of 0.1 mV). Between the 2 areas of scar tissue a narrow, pathway of slow conduction was present. Bipolar electrograms recorded from within this channel showed low amplitude fractionated deflections of prolonged duration. Transsection of this crucial pathway of conduction delay by constructing a linear lesion between the 2 non-conductive structures resulted in termination of IART.
ICV: inferior caval vein

Macro-Reentrant Tachycardia

Twenty-seven activation maps revealed an IART (CL = 316 ± 78 (210-515) ms). Crucial pathways of conduction targeted for ablation were characterized by fractionated potentials in all patients.

The activation map in **Figure 1** shows an example of an IART (CL = 324 ms). The wavefront circulated around a large area of scar tissue. Between these two areas, a narrow pathway of slow conduction was present. Bipolar electrograms recorded at this area consisted of low amplitude, fractionated potentials. Transsection of this corridor by constructing a linear lesion between 2 non-conductive structures resulted in termination of IART.

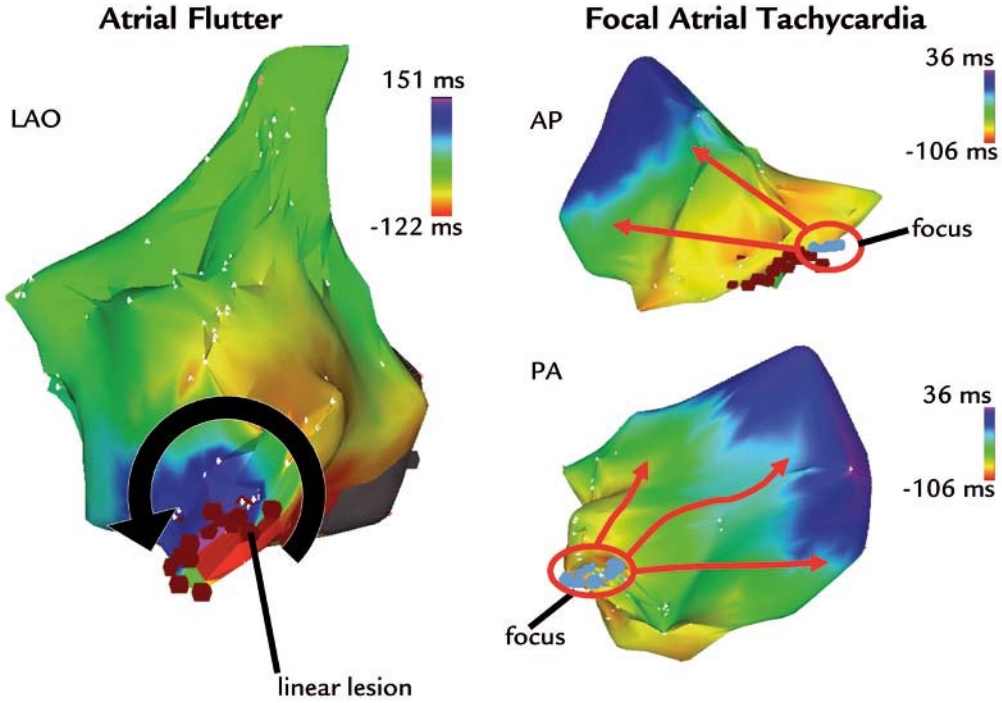

Figure 2.

AFL and FAT in a patient who had an atrial switch procedure. The color coded activation map of the right atrium showed a counterclockwise rotation of the activation wavefront around the tricuspid valve (left panel). After creation of a conduction block over the cavo-tricuspid isthmus (red dots), FAT appeared (right panel). The FAT activation map showed a focal activation pattern originating from an area nearby the ablation line. Area ablation (blue dots) was performed resulting in termination of FAT. The tricuspid valve was omitted for purpose of visualization.

LAO = left anterior oblique, AP = antero-posterior, PA = postero-anterior view, EA = bipolar potential at site of earliest endocardial activity.

Crucial pathways of conduction delay were found between areas of scar (n = 15) or between the lateral right atriotomy scar and the inferior caval vein (n = 5). In one patient with a Fontan circulation, a linear lesion was created between the right atrio-pulmonary conduit and scar tissue. In one patient with atrial septal defect repair, a lesion was created between the ASD-patch and the tricuspid valve. In patients after Mustard's procedure, ablation was performed in the pulmonary venous atrium between the left atrial roof and the right atriotomy scar (n = 4). In one patient, the critical zone of conduction was found between the coronary sinus os and the systemic venous baffle. Ablation resulted in termination of 19 (70%) AT; 8 AT (30%) did not terminate during ablation.

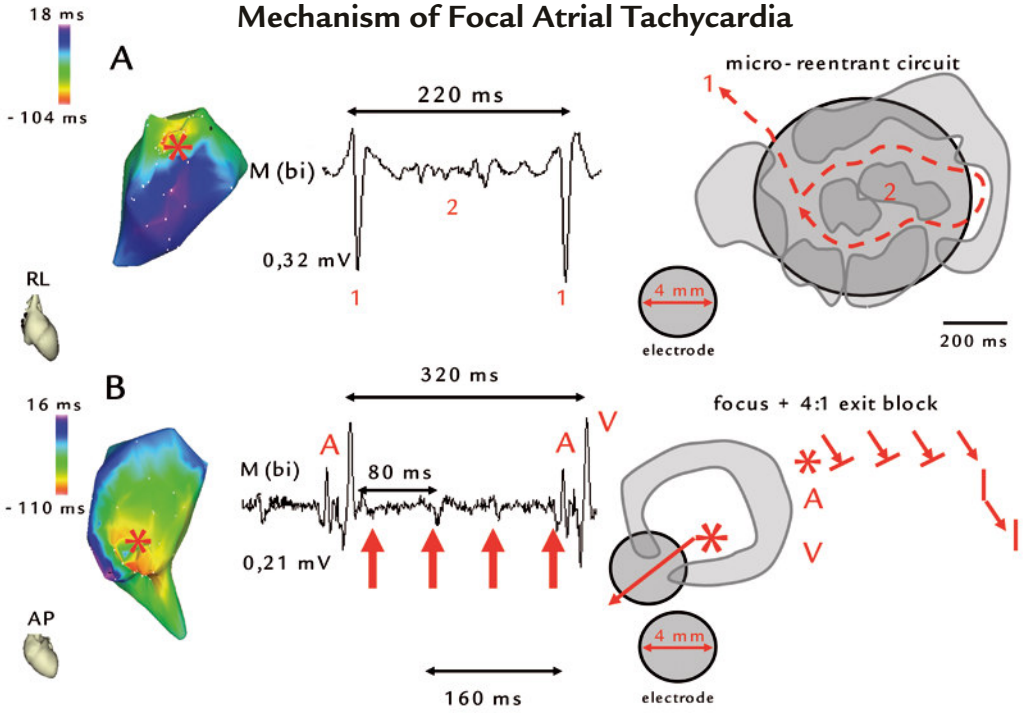

Figure 3.
Right atrial activation maps demonstrating 2 different FAT present in a patient with congenital corrected transposition of the great arteries (CL FAT1 = 220 ms panel A, FAT2 = 320 ms panel B). Panel A: The electrogram recorded at the site of earliest activity located at the high antero-lateral wall consisted of continuous electrical activity. Panel B: The activation map and the electrogram recorded at the site of origin of this FAT, is indicative for the presence of a focus with a 4:1 intra-atrial conduction block. See text for explanation. RL = right lateral, AP = antero-posterior view, M(bi) = electrogram recorded from the site of origin.

Focal Atrial Tachycardia

In 8 patients, activation maps constructed during tachycardia revealed a focal pattern of activation (CL = 359 ± 93 (200-500) ms). Ten different FAT were recorded. FAT appeared after ablation of AFL in 2 patients and after termination of IART in one.

In Figure 2, different activation maps recorded in a patient with transposition of the great arteries corrected with a Mustard followed by a Jatene procedure are shown. This patient presented with incessant AT and the right atrial activation map showed a typical counter-clockwise AFL (CL = 275 ms). Construction of a linear lesion (red dots) at the cavo-tricuspid isthmus resulted in termination of AFL. However, a second AT spontaneously appeared. Mapping of this AT (CL = 500 ms) revealed FAT. The activation wavefront originated from the lower intra-atrial septal area. Area ablation of this region (blue dots) resulted in resumption of sinus rhythm.

In another patient with congenital corrected transposition of the great arteries, 2 different FAT were inducible (Figure 3). The first activation map (panel A) revealed a focal pattern of activation (CL = 220 ms) originating from the high antero-lateral atrial wall. The bipolar electrogram (M(bi)) recorded at the site of earliest endocardial activity, consisted of relatively large atrial potentials (0,32mV). Between these potentials, continuous electrical activity was recorded suggestive of a micro-reentrant mechanism (upper right panel).

The second activation map (panel B) also showed a focal activation pattern (CL = 320ms), now arising from the lower anterior atrial wall. Again, large atrial potentials were recorded. However, the bipolar electrogram recorded at the site of earliest activation contained low amplitude potentials with an interval of 80ms. This recording was suggestive for the presence of a source nearby the mapping electrode with a 4:1 intra-atrial block to the atrium, as demonstrated in the schematic drawing in the lower right panel. The spatial resolution, however, is limited due to the diameter of the recording electrodes and the inter-electrode distance of the mapping catheter and therefore precludes a final conclusion on the FAT mechanism.

Other examples of abnormal electrograms recorded at the site of origin of FAT in patient with an atrial septal defect and atrio-ventricular septum defect are shown in respectively the upper and lower panel of Figure 4. In panel A, a FAT (CL = 500 ms) originated from the low posterior wall of the right atrium (although theoretically a macro-reentry mechanism with a zone of extremely slow conduction might have caused this arrhythmia). The activation wavefront radially spreaded from the site of origin but was partly blocked in the caudal direction. The electrogram recorded at the site of earliest endocardial activity showed low amplitude (0,27mV), fractionated potentials with a duration of 244ms. Area ablation of this site resulted in termination and non-inducibility of FAT.

In panel B, an activation wavefront (CL = 220 ms) arose from the high postero-septal region. At this site, a small area could be delineated from which only fractionated potentials were recorded (pink dots). Area ablation, aimed at encircling the entire area containing

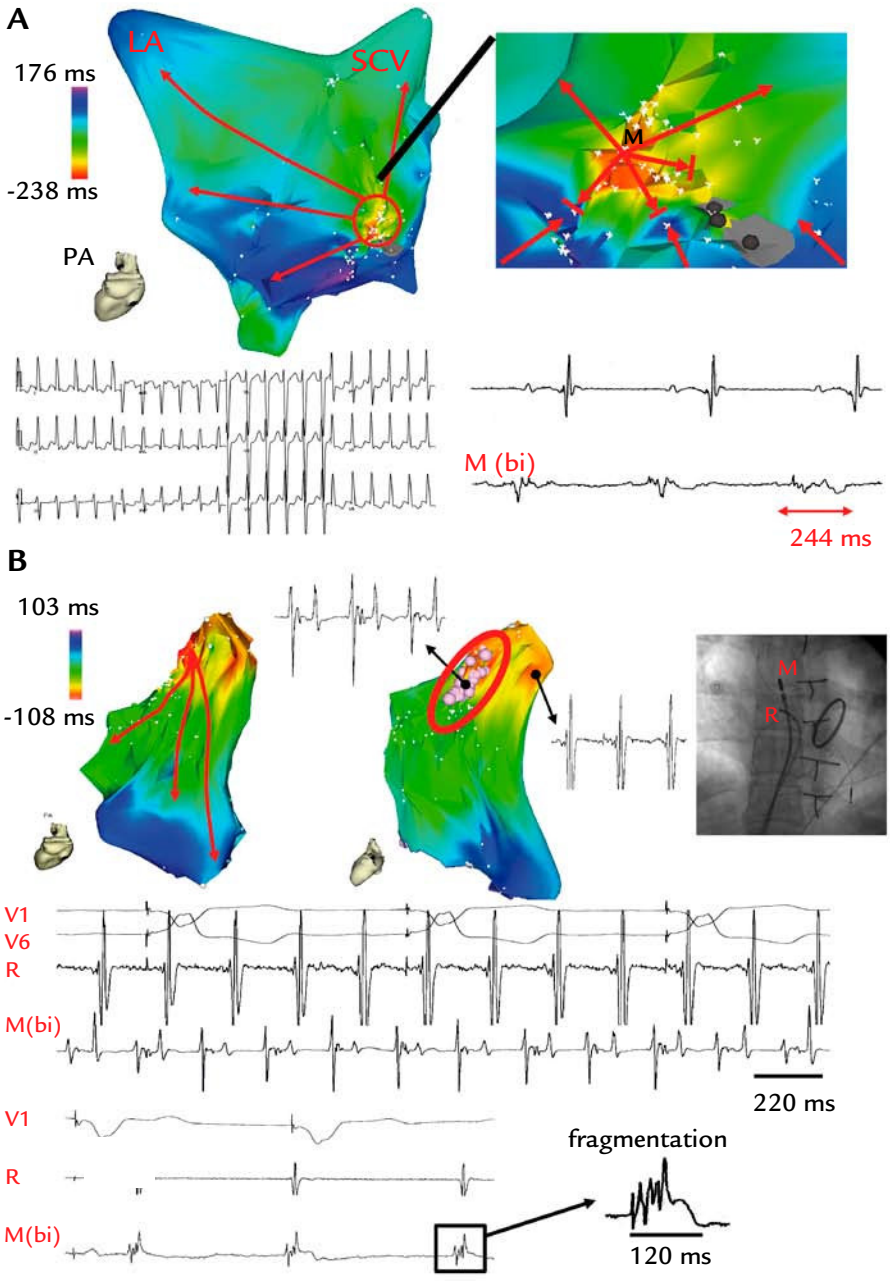

Figure 4.

Panel A: Activation map (left panel) demonstrating a possible FAT originating from the lower posterior right atrial wall. The right panel showed recordings from the site of origin. The electrogram recorded (M (bi) at the successful ablation site consisted of fractionated, low amplitude potentials. *Panel B:* FAT originating from the high postero-septal region. An area (length = 2cm) from which fractionated potentials were recorded was accurately delineated. After ablation (pink dots), fractionated electrograms were recorded during sinus rhythm within this lesion (M (bi).

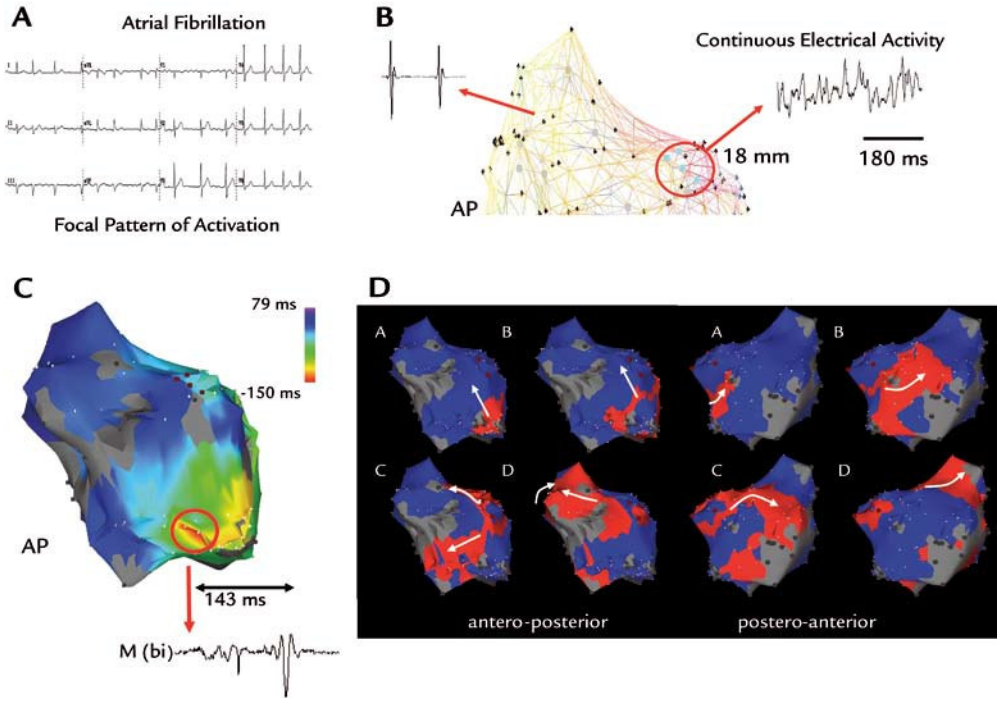

Figure 5.
Fontan patient presented with AF (panel A) at the onset of the procedure. A circumscriptive area (diameter = 18mm) from which continuous electrical activity was recorded was found in the septal region (panel B). Ablation at this site terminated AF and a regular AT with a focal activation pattern appeared (panel C). The propagation maps (panel D) showed 2 large wavefronts emerging from the site of earliest activity propagating over the anterior and posterior wall and finally fusing in the upper part of the right atrial free wall. AP = antero-posterior view, M (bi) = bipolar electrogram.

fractionated potentials, resulted in termination of FAT. Prior to ablation, the electrograms recorded from this area during sinus rhythm also contained fractionated potentials.

Focal Atrial Fibrillation

Interestingly, whereas in most patients the surface ECG during AT showed a regular atrial rhythm, a surface ECG typical of atrial fibrillation (AF) was present in 2 patients (**Figures 5 and 6**). However, in both patients, detailed mapping revealed a focal mechanism giving rise to fibrillatory conduction.

A patient with a tricuspid atresia palliated with a Fontan procedure presented with "AF" at the onset of the procedure (**Figure 5** panel A). Surprisingly, during tachycardia, large parts of the atrium were activated in a regular manner. However, a circumscribed area at the postero-septal wall was accidentally encountered exhibiting continuous local electrical activity (panel B). Application of RF-energy at this area terminated "AF" but another regular AT (CL = 245 ms, panel C) appeared. Mapping of this AT revealed a focal pattern

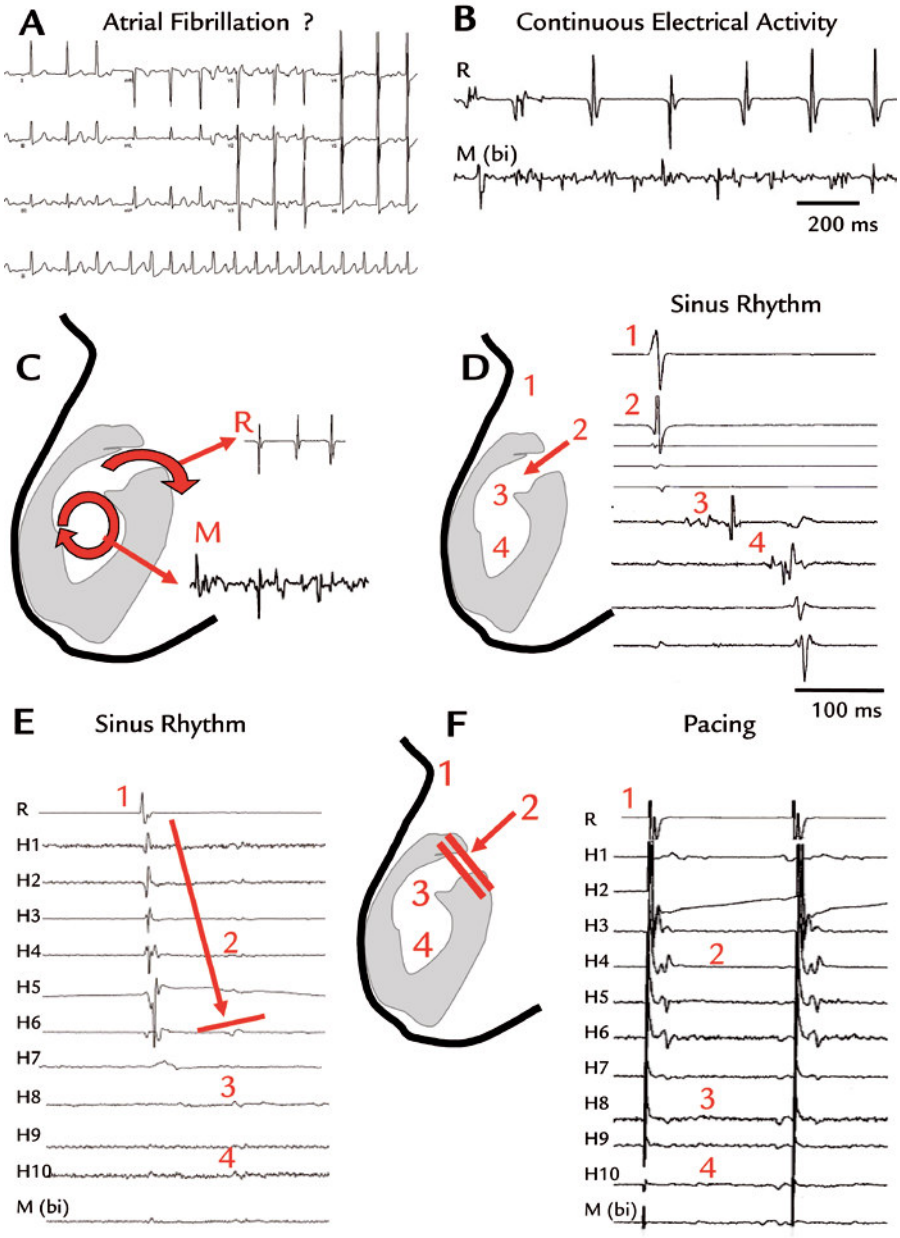

Figure 6.

Continuous electrical activity recorded during AF (panel A). Mapping during AF revealed an area of continuous electrical activity at the right atrial free wall (panels B, C). AF converted spontaneously to SR. During SR at this site (panel D, recording 3) a prolonged, fractionated potential (130ms) filling the gap between the early activated high right atrial free wall and the late activated lower part of the right atrium was recorded. This activation pattern was the result of slow conduction through a narrow pathway bordered by scar areas (gray color). Ablation was targeted at the entrance site. After ablation, electrical activity in the scar embedded region disappeared (panels E, F). Electrograms were recorded with a 20-electrode catheter.

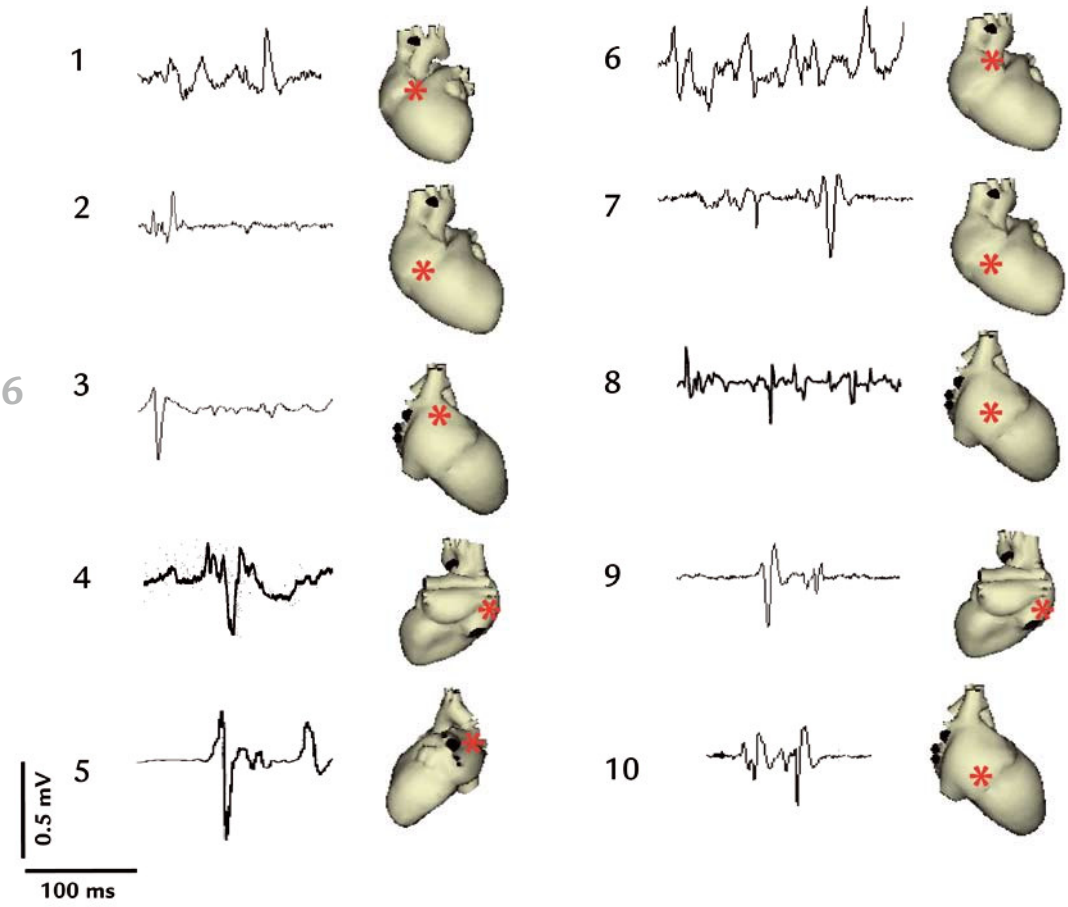

Figure 7.
Bipolar electrograms recorded at the site of earliest activation of all ten AT of focal origin. The red asterix on the schematic representation of the heart indicates the site of origin.

of activation originating from the caudal part of the atrium (panel D). The electrogram recorded at the site of earliest endocardial activity consisted of fractionated potentials (duration 143ms). Electrograms recorded from the surrounding tissue had a higher amplitude (>0.5mV) and a shorter duration (<70 ms). Ablation at this earliest activated site resulted in termination of FAT and resumption of sinus rhythm.
Fibrillatory conduction originated from a small, partly isolated, atrial area in the other AF patient (**Figure 6**). This area, exhibiting low amplitude fractionated electrical activity was responsible for maintenance of the arrhythmia. During sinus rhythm, a fractionated electrogram (panel D, signal 3, duration 130 ms) filled the gap between the early activated high right atrial free wall and the late activated lower part of the right atrium. This pattern

of activation was most likely the result of slow conduction through a narrow pathway of conductive tissue bordered by areas of non-conducting tissue (scar tissue). By complete electrical isolation (as demonstrated by the absence of activity after ablation) of this area the tachycardia terminated and was non-inducible after ablation. In all patients, ablation of the earliest activated region during AT resulted in termination of FAT. Electrogram characteristics of all AT of focal origin and the site of origin are summarized in **Figure 7**.

Discussion

This study demonstrated that areas of abnormal conduction, in patients after surgery for CHD, may not only serve as a crucial pathway of slow conduction which is part of a large reentrant circuit or but also as the site of origin of a focal atrial arrhythmia.
As post-operative AT in CHD patients are often associated with increased morbidity and anti-arrhythmic drugs are only of limited value, catheter ablation may serve as an alternative treatment modality. However, in order to reveal the underlying mechanism and to depict successful ablation sites, detailed endocardial activation mapping guiding the ablation procedure is mandatory.

Macro-Reentrant Tachycardia

In line with other studies, the majority of AT was caused by a cavo-tricuspid dependent AFL or macro-reentrant mechanism involving areas of dense scar.[5;8;11-14] In this patient group, extensive cardiac surgery and hemodynamic overload results in large areas of scar tissue often diffusely spread throughout the atria. Surviving myocardial fibers embedded within scar areas play a key role in the induction and perpetuation of AT. As multiple pathways through areas of scar tissue often exist, different AT may co-exist. It was demonstrated that these different AT often have a common crucial pathway of conduction and that ablation of this pathway abolished all AT. [2]
Except for 3 patients after Mustard's procedure, the arrhythmogenic substrate was located in the right atrium. A right atrial arrhythmogenic substrate is likely associated with the presence of an extensive atriotomy scar and atrio-pulmonary conduits in a large number of patients. Additionally, it has been shown that especially in patients with tricuspid atresia the right atrial myocardial architecture is affected.[15]

Focal Patterns of Activation

In a significant number of patients, focal patterns of activation were observed. To the best of our knowledge, reports on FAT in CHD patients are rare and the presence of multiple FAT have so far not been reported. Reithmann et al. described the presence of FAT in one patient after type II ASD repair and in one patient with Ebstein's anomaly who underwent cardiac surgery for an accessory pathway.[16] In both cases, the site of origin of FAT was located near surgically created barriers. This was also reported by Kanter et al. who described the presence of FAT in 2 patients with transposition of the great arteries, after Mustard's procedure.[17] The origin of FAT was located adjacent to suture lines in both the pulmonary and systemic venous atrium. In the current study, FAT did not only arise from sites nearby surgically created barriers or from sites which are a known predilection sites of FAT in patients with normal hearts.[18]

It has been postulated that FAT may originate from areas with enhanced non-uniform anisotropic properties. Poor cell-to-cell coupling result in diminished electrotonic inhibition thereby allowing a rapidly discharging focus to become apparent.[19;20]
In the current study, during FAT, fractionated, low amplitude potentials and continuous electrical activity were recorded from the earliest activated sites. Furthermore, during sinus rhythm these sites exhibited fractionated electrograms supportive for the presence of structural abnormalities at the site of FAT origin. As areas of scar tissue are diffusely spread throughout the atria in CHD patients, FAT can theoretically develop from numerous sites. With regard to the underlying mechanism of FAT, due to the lack of spatial resolution of the mapping catheter, a final conclusion cannot be drawn. The recording of continuous electrical activity during some AT could indicate the presence of a micro-reentrant circuit. On the other hand, it is known from experimental studies that triggered activity may cause AT in response to pacing or stretch.[21]
Interestingly, the current study demonstrated that a surface electrogram resembling AF is the result of focal activity giving rise to fibrillatory conduction. Therefore, in CHD patients, given the necessity of maintaining sinus rhythm, it may be recommendable to perform endocardial mapping to exclude the possibility of focal activity in case of recurrent AF.

Recording Techniques

Mapping was performed with the 3-D electro-anatomical mapping system (CARTO) in all patients. Bipolar electrograms were used for construction of activation / voltage maps. In a previous study, we demonstrated that in patients with CHD, bipolar recordings are preferable, as they allow voltage based scar tissue delineation and are less susceptible to noise or far-field potentials.[4;5] In addition, Weiss et al. demonstrated that annotation of the earliest onset of the bipolar electrogram provides an efficacious guide for location of the FAT origin.[22] In case of a macro-reentrant tachycardia, 3-D reconstruction of the atria allow visualization of complex reentrant pathways thereby facilitating selection of suitable target sites for ablation. In case of a FAT, the wavefront propagates away from one single region. The activation map does not reveal a wavefront circulating around a macroscopic anatomical structure or a structural/functional line of conduction block. Hence, "macroscopic" is thus determined by the size of the mapping electrode.

Study Limitations

As this study was not focused on the underlying mechanism of FAT, we did not use pacing manoeuvres or pharmacological testing to distinguish between the different underlying mechanisms. Furthermore, high density mapping at the site of origin of FAT was limited by the diameter of the mapping electrode and a reentrant circuit with a diameter smaller than the inter-electrode distance of the mapping electrode could therefore have been missed.

Conclusion

AT in patients with surgically correct CHD is caused by a macro-reentrant mechanism in most patients, however AT is caused by a focal mechanism in some patients. Areas of abnormal conduction may be the crucial pathway within a large reentrant circuit, but they may also be the site of origin of a focal atrial tachycardia and thus play an important role in the pathogenesis of these AT. Catheter ablation directed at areas of abnormal conduction ("source ablation") is effective in patients with CHD with post-operative FAT.

References

1. Triedman JK. Arrhythmias in adults with congenital heart disease Heart. 2002;87:383-389.
2. Delacretaz E, Ganz LI, Soejima K, Friedman PL, Walsh EP, Triedman JK, Sloss LJ, Landzberg MJ, Stevenson WG. Multiple atrial macro-re-entry circuits in adults with repaired congenital heart disease: Entrainment mapping combined with three-dimensional electroanatomic mapping. Journal of the American College of Cardiology. 2001;37:1665-1676.
3. Van Hare GF, Lesh MD, Ross BA, Perry JC, Dorostkar PC. Mapping and radiofrequency ablation of intraatrial reentrant tachycardia after the Senning or Mustard procedure for transposition ofthe great arteries. Am J Cardiol. 1996;77:985-991.
4. de Groot NM, Schalij MJ, Zeppenfeld K, Blom NA, Van der Velde ET, van der Wall EE. Voltage and activation mapping: how the recording technique affects the outcome of catheter ablation procedures in patients with congenital heart disease. Circulation. 2003;108:2099-2106.
5. de Groot NM, Kuijper AF, Blom NA, Bootsma M, Schalij MJ. Three-dimensional distribution of bipolar atrial electrogram voltages in patients with congenital heart disease. Pacing Clin Electrophysiol. 2001;24:1334-1342.
6. Gepstein L, Hayam G, Ben Haim SA. A novel method for nonfluoroscopic catheter-based electroanatomical mapping of the heart. In vitro and in vivo accuracy results. Circulation. 1997;95:1611-1622.
7. Gepstein L, Evans SJ. Electroanatomical mapping of the heart: basic concepts and implications for the treatment of cardiac arrhythmias. Pacing Clin Electrophysiol. 1998;21:1268-1278.
8. Saoudi N, Cosio F, Waldo A, Chen SA, Iesaka Y, Lesh M, Saksena S, Salerno J, Schoels W. A classification of atrial flutter and regular atrial tachycardia according to electrophysiological mechanisms and anatomical bases – A statement from a Joint Expert Group from the Working Group of Arrhythmias of the European Society of Cardiology and the North American Society of Pacing and electrophysiology. European Heart Journal. 2001;22:1162-1182.
9. Lesh MD, Kalman JM, Saxon LA, Dorostkar PC. Electrophysiology of «incisional» reentrant atrial tachycardia complicating surgery for congenital heart disease. Pacing Clin Electrophysiol. 1997;20:2107-2111.
10. Triedman JK, Jenkins KJ, Colan SD, Saul JP, Walsh EP. Intra-atrial reentrant tachycardia after palliation of congenital heart disease: characterization of multiple macroreentrant circuits using fluoroscopically based three-dimensional endocardial mapping. J Cardiovasc Electrophysiol. 1997;8:259-270.
11. Anne W, van Rensburg H, Adams J, Ector H, Van de WF, Heidbuchel H. Ablation of post-surgical intra-atrial reentrant tachycardia. Predilection target sites and mapping approach. Eur Heart J. 2002;23:1609-1616.
12. Nakagawa H, Shah N, Matsudaira K, Overholt E, Chandrasekaran K, Beckman KJ, Spector P, Calame JD, Rao A, Hasdemir C, Otomo K, Wang Z, Lazzara R, Jackman WM. Characterization of reentrant circuit in macroreentrant right atrial tachycardia after surgical repair of congenital heart disease: isolated channels between scars allow «focal» ablation. Circulation. 2001;103:699-709.
13. Nakagawa H, Jackman WM. Catheter ablation of macroreentrant atrial tachycardia in patients following atriotomy. Eur Heart J. 2002;23:1566-1568.
14. Dorostkar PC, Mackall JA, Wiseman MN, Scheinman MM. Electroanatomic mapping as a supportive tool to map complex postoperative atrial reentrant tachycardias in patients with congenital heart disease. Journal of Electrocardiology. 2000;33:147.
15. Ho SY, Anderson RH, Sanchez-Quintana D. Atrial structure and fibres: morphologic bases of atrial conduction. Cardiovascular Research. 2002;54:325-336.
16. Reithmann C, Hoffmann E, Dorwarth U, Remp T, Steinbeck G. Electroanatomical mapping for visualization of atrial activation in patients with incisional atrial tachycardias. European Heart Journal. 2001;22:237-246.
17. Kanter RJ, Papagiannis J, Carboni MP, Ungerleider RM, Sanders WE, Wharton JM. Radiofrequency catheter ablation of supraventricular tachycardia substrates after mustard and senning operations for d-transposition of the great arteries. J Am Coll Cardiol. 2000;35:428-441.
18. Chen SA, Tai CT, Chiang CE, Ding YA, Chang MS. Focal atrial tachycardia: reanalysis of the clinical and electrophysiologic characteristics and prediction of successful radiofrequency ablation. J Cardiovasc Electrophysiol. 1998;9:355-365.

19. Joyner RW, Wang YG, Wilders R, Golod DA, Wagner MB, Kumar R, Goolsby WN. A spontaneously active focus drives a model atrial sheet more easily than a model ventricular sheet. Am J Physiol Heart Circ Physiol. 2000;279:H752-H763.
20. Lesh MD, Kalman JM, Olgin JE. New approaches to treatment of atrial flutter and tachycardia. J Cardiovasc Electrophysiol. 1996;7:368-381.
21. Fenelon G, Stambler BS. Focal Origin of Atrial Tachycardia in Dogs with Rapid Ventricular Pacing-Induced Heart Failure. J Cardiovasc Electrophysiol. 2003;14:1093-1102.
22. Weiss C, Willems S, Rueppel R, Hoffmann M, Meinertz T. Electroanatomical mapping (CARTO (R)) of ectopic atrial tachycardia: Impact of bipolar and unipolar local electrogram annotation for localization the focal origin Journal of Interventional Cardiac Electrophysiology. 2001;5:101-107.